



Laboratory testing and numerical modelling of frame apex connections fabricated from steel cold-formed sections

Sherif A. Mourad¹, M. T. Hanna², Hazem H. Elanwar³, Mohamed H. Zaki⁴

Abstract

In the recent years, the use of cold-formed steel sections in construction has significantly risen. Therefore, it was essential to carry out several studies to test the behavior and strength of structures composed of steel cold-formed sections under several cases of loading since their behavior is different from that made of conventional steel sections. In this study, the behavior of cold formed steel gable frame apex connection subjected to major axis bending moments is investigated. For this purpose, experimental and numerical models were developed. Two types of fasteners were studied. First, self-drilling screws with 6 mm diameter, whereas, the second type is ordinary bolts of grade 4.4 and 12 mm diameter. Both beams and columns were made of lipped channel sections of web height, flange width, lip and thickness of 200, 60, 20, and 2 mm, respectively. Four specimens were fabricated to investigate the behavior of these connections. The main parameters were the thickness of the gusset plate, the use of upper and lower flange plates, and the different fastener types. The specimens were modeled numerically using finite element software. Shell elements were used to model the members, while fasteners were modeled using wire elements. The experimental results were used to verify and fine-tune the numerical model. The study showed that the dominant mode of failure was the local buckling of gusset plates. Increasing the thickness of gusset plate results in a significant increase in the ultimate load carrying capacity of apex connection as well as the connection ductility and energy dissipation. The use of upper and lower flange plates increased the flexural capacity of apex connection. In-addition, failure of cross-section was rarely noticed outside the gusset plate.

1. Introduction

Recently, Cold-Formed Sections (CFS) have emerged as an alternative to traditional hot rolled profiles that is typically used for low-rise and mid-rise buildings. CFS has the advantage of small thicknesses and hence, they provide economic and light weight profiles. Design using CFS profiles has been adopted in various standards such as the American Iron and Steel Institute

¹ Professor, Faculty of Engineering, Cairo University, Egypt < smourad@eng.cu.edu.eg >

² Professor, Housing and Building National Research Center, Egypt <maged.tawfick@hbrc.edu.eg>

³ Associate Professor, Faculty of Engineering, Cairo University, Egypt <hazem_alanwar@eng.cu.edu.eg >

⁴ Teaching Assistant, Faculty of Engineering, British University in Egypt <Mohmed. Hosni@bue.edu.eg>

standards AISI-S100-12, and the European Code EC3: Part 1-3. Although buildings using CFS is getting more attention, yet, some types of structures such as portal frames are not comprehensively developed yet. One of the main challenges of portal frames using CFS is the behavior of eave and apex moment connections. Previous studies were carried out to investigate the member and the connection behavior of portal frames using CFS. Calderoni et al. (2009) showed through experimental investigation that local buckling governed and reduced the beam resistance significantly when subjected to cyclic and static loading. Moreover, finite element models were developed to investigate the CFS beam bending behavior and it was capable of providing relatively accurate estimate (2018). Meza et al. (2018) carried out experimental work to determine the cross-sectional capacity of cold-formed steel built-up columns with four different cross-sectional geometries and assembled with either bolts or self-drilling screws and flat plates of different thicknesses. The experimental results revealed that spacings between connectors has a remarkable impact on the observed buckling mode. On the other hand, connector spacing did not affect the cross-sectional capacity.

There are various studies focusing on the investigation of the behavior of CFS portal frame connections. Tshuma & Dundu (2017) investigated the strength and behavior of column-to-rafter internal connections. The most essential objective of this research is to estimate the capacity and failure modes used connections, as well as the behavior of the connected members. Hanna et al. (2018) investigated the beam-column moment connections. Two different gusset plate configurations were tested, tapered gusset plate and rectangular gusset plate. Rasmussen (2018) investigated the different portal frame connections (Corner or eave, apex, and base connections) of cold-formed steel sections through experimental testing and FE models. The study showed that two failure modes dominate the failure of eaves connection: fracture of screws and gusset plate bending. For apex connection, the dominant failure mode was local buckling of compression part of gusset plate. Blum et al. (2019) showed that the base connection had remarkable influence on long span portal frames subjected to lateral loads. El-Hadary et al. (2019) investigated the different bolted connection configurations in cold-formed steel frames. The analysis indicated that the dominant failure modes were local buckling of gusset plate, local buckling of C-sections, and bearing failure in C-sections and gusset plate. Moreover, the suitable choice of bolts' arrangement is proven to have significant impact on the ultimate moment capacity. Lim & Nethercot (2018) carried out a study to predict the stiffness of bolted moment-connections between cold-formed steel members through experimental testing and numerical modelling of apex connections. Elkersh (2018) used experimental and numerical modelling to assess the frame apex bolted connections for various plate thicknesses and different bolts arrangements. It was shown that the gusset plate thickness governs the ultimate load capacity of the apex connection. Öztürk and Pul (2018) showed the impact of different parameters such as distance between ends of beams and using apex plate with and without stiffener. Blum and Li (2019) investigated the stability of apex connections for various rafter depth and thickness of cold-formed steel portal frame. Chen et al. (2021) extended the studies to included material non-linearity, geometric imperfections, and bolt bearing behavior. Furthermore, it is essential to study the behavior of CFS connections using self-drilling screws. Roy et al. (2018) carried out experimental investigation and finite element modelling to study the effect of different configurations of connections using self-drilling screws for cold-formed steel with high strength. Number of screws, screw diameter, screw spacing, and edge distance were the main parameters to be tested. The obtained experimental results were verified against a non-linear finite element model. The comparison of the two approaches came up with acceptable

similarities in terms of strength and behavior of the screwed connections. Badr et al. 0 carried out experimental and numerical investigations on cold-formed walls sheathed by Fiber-Cement Board (FCB) under monotonic lateral load using self-drilling screws to connect the FCB and the steel framing members. In order to model the screws for numerical model, mesh independent fasters are used. This approach proved to be efficient and showed good agreement with experimental behavior. Huynh et al. (2020) carried out experimental evaluation on screwed connections using self-drilling screws to connect cold-formed steel sheets. The targeted criteria to be evaluated is the shear capacity and failure of screws. The main variables were types of screws, various thicknesses of steel sheets to test the behavior regarding self-drilling screwed connections bearing and tilting.

The previous research contributed to the advancement of CFS utilization in portal frames. However, further studies are needed to assess behavior and capacity of CFS apex connections. In this paper, four experiments were conducted to assess apex moment connection in CFS aiming to enhance its response and to compare it to the member's bending capacity. To investigate various connections configuration, the finite element software, ABAQUS (2011), is used to develop a numerical model verified against the experimental results. Hence, a parametric study is performed changing different parameters such as gusset plate thickness, spacing and number of screws. After that, the impact of changing each parameter is evaluated against the member's moment capacity.

2. Experimental Investigation

2.1 Details of specimens

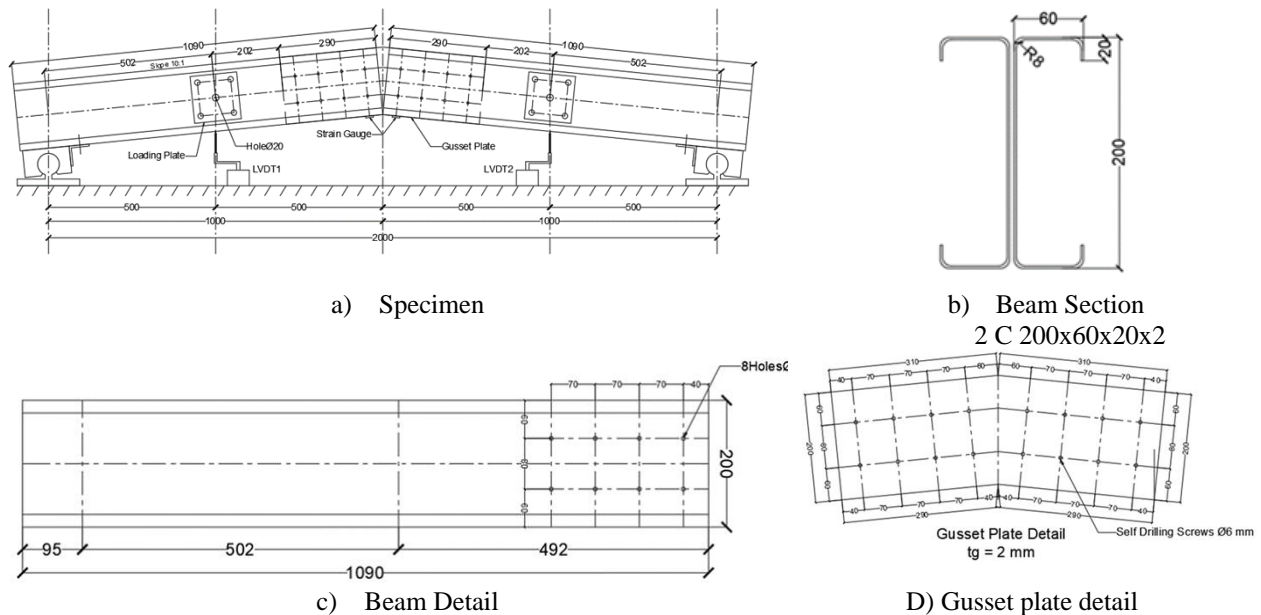


Figure 1: Tested Specimens Details

Four specimens were tested. The profiles used is a back-to-back double lipped channel (C) with height 200 mm, flange depth 60 mm, lip depth 20 mm and thickness 2 mm. Each of the four

specimens is formed by connecting two beams with slope 1:10 and length 1090 mm to each other using gusset plate at the apex. The points of load application are determined to be at 500 mm horizontally from the apex. The first two specimens SDS1, SDS2 are connected using 6mm diameter screws as fastener, however, specimens OB1, OB2 are connected using 12 mm diameter ordinary bolts (grade 8.8, $F_u=800\text{MPa}$, $F_y=640\text{MPa}$) as fasteners. For SDS1 as well as OB1, only gusset plate is used to connect the web of the two beams, while SDS2, and OB2 have upper and lower plates connecting the cross section flanges besides the web gusset plate. Details of the specimens are shown in Fig. 1, and listed in Table 1.

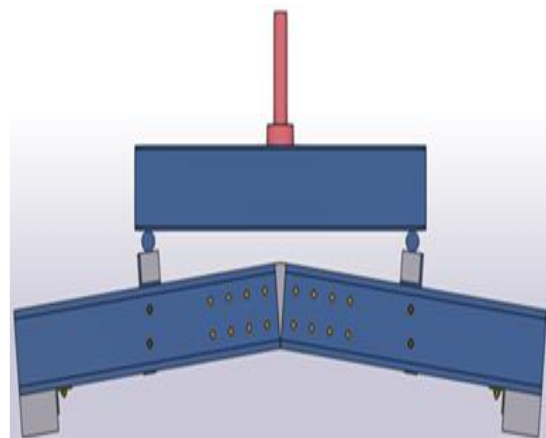
Table 1. Details of test specimens

	Connector Type	Connector Diameter (mm)	Maximum Load (KN)	Moment Capacity (KN.m)	Deflection at Max load (mm)	Failure
SDS1	Self-drilling Screws	6	18.45	2.23	9.45	Local Buckling of Gusset Plate
SDS2	Self-drilling Screws	6	27.7	3.42	4	Local Buckling of Upper Flange Plate followed by buckling of Gusset Plate
OB1	Ordinary Bolts	12	29.7	3.59	6.3	Local Buckling of Gusset Plate
OB2	Ordinary Bolts	12	39.3	4.57	7.4	Local Buckling of Upper Flange Plate followed by buckling of Gusset Plate

In order to obtain the mechanical properties of cold-formed steel used, group of specimens with 3 tensile coupons were extracted from apex plates and rafter profiles. The testing specifications conforms to the ASTM A370 (2006) “Standard Test Methods and Definitions for Mechanical Testing of Steel Products”. the average values of yield stress and ultimate stress for both beams and gusset plates are 350 MPa and 450 MPa; respectively. Young’s modulus (E) is taken 210,000 MPa.



a) Test setup



b) Loading technique

Figure 2: Test setup and loading technique

The proposed test setup is shown in Fig. 2. The loading device was employed to apply the ultimate load at two points on the rafters with distance 500 mm from the center of the gusset plate. The load coming from the hydraulic jack is distributed to the two points through I-shaped rigid beam strengthened with steel rods along its length. The boundary conditions used at the two ends are hinged supports using equal angles connected to the beams using 12 mm ordinary bolts and rested on the support that is fixed to the ground to restrict any vertical or horizontal movements. The proposed loading technique is illustrated in Fig. 2. It can be noticed that the load is directly applied on the upper flange using transfer beam rested on steel rod. The beam cross-section, at support locations, is strengthened with vertical steel plate welded to the two channel lips besides using wooden blocks as stiffeners along web height. Moreover, at points of load applications, wooden blocks are used as stiffeners to avoid web buckling and crippling. In order to control the out-of-plane movements, lateral supports are used just after the supports and at location of apex connection. In addition, two linear variable displacement transducers (LVDT) are used under the two points of load application to measure the vertical displacement of each point. The loading technique used for all specimens is displacement control technique. A hydraulic jack with 50 ton capacity was used to apply monotonic gravity load.

2.2 Test Results

The developed bending moment, M , was normalized with respect to the section flexural capacity, M_c , and the ratio M/M_c is drawn versus the relative rotation of the connection in Fig. 2. Note, the section flexural capacity, M_c , was determined according to AISI (2012) and is equal to 9.47 KN.m.

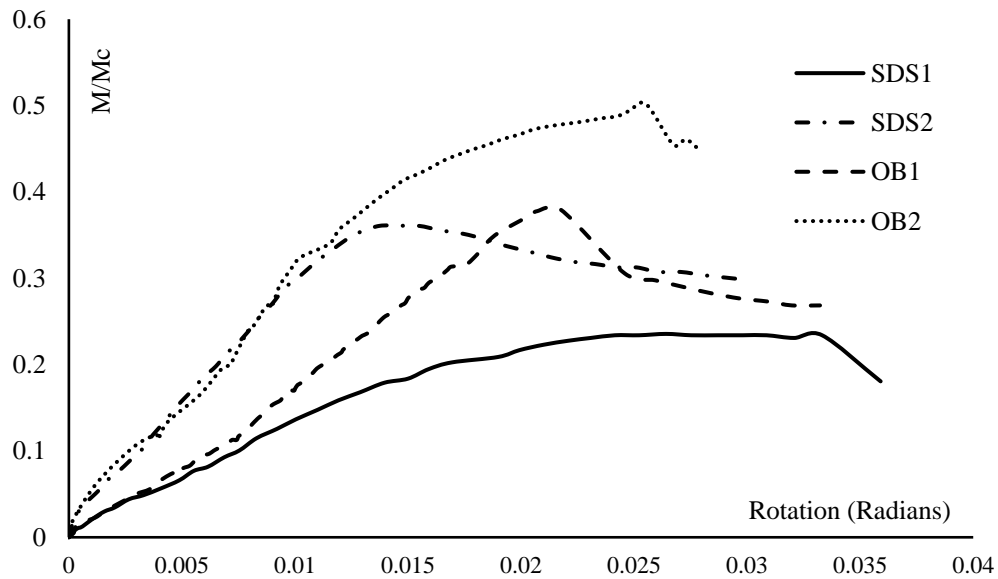


Figure 3: Experimental M/M_c versus connection rotation angle.

For specimens SDS1, OB1, the ultimate M/M_c ratios recorded were 24%, 38%; respectively. The dominant failure mode was local buckling of gusset plate connecting the two beams to each other without any failure noticed in the fasteners. The vertical displacement of SDS1 at ultimate moment was 9.45mm, while for OB1, the vertical displacement at ultimate loads was 6.3mm.

However, in specimens SDS2, and OB2, the failure initiated as local buckling of the upper flange plate located in compression zone and then moved to the compression side of apex gusset plate. The ultimate M/M_c ratios for specimens SDS2, and OB2 were 36%, and 50% respectively. The vertical displacement of specimen SDS2 at ultimate load was 4mm, while for specimen OB2, this value was 7.4mm. The failure modes of the tested specimens are depicted in Fig. 7 and Fig. 8.

3. Finite Element model

The tested specimens have been simulated numerically using ABAQUS (2011) software. The cold formed beams as well as the connecting plates have been modeled using shell elements of type S4R with maximum mesh size of 10 mm by 10 mm. The degrees of freedom at each node of this element are three in translational U_x , U_y , U_z and three in rotational Θ_x , Θ_y , Θ_z . The cold-formed steel sections are modeled as isotropic elastic material with Young's modulus $E = 210,000$ MPa and Poisson's ratio $\nu = 0.3$. A bi-linear stress-strain relation has been used with yield stress, $F_y=350$ MPa. In order to simulate the hinged boundary conditions, coupling constraint is assigned to the point at the middle height of the section web where restraints should be assigned. After that, the Z-axis rotation is released while the other DOFs are restrained. Lateral restraints are assigned at the locations that are laterally supported in the experimental setup. To apply the gravity loads on the two points, the point of loading in the upper flange is assigned with a coupling constraint. Then, displacement-controlled gravity load is applied at the reference node located at the center of the coupling constraint.



Figure 4: Finite element model.

Bolted connections are defined as point-based fasteners with Cartesian section as connector type. On the other hand, self-drilling screws are modeled as wires connecting attachment points in each element using Cartesian section as connector type. Cartesian section provides a connection between two nodes that allows translational behavior in three local Cartesian directions. This definition of self-drilling screws is previously used by Badr, A. R. (2019) and proved to be efficient and showed good agreement with experimental behavior. In order to model the surface contact between the different elements, a surface-to-surface contact is assigned to these elements using frictionless tangential behavior, while the normal behavior is defined as hard contact. Details of the experimental setup as well as the developed finite element model are illustrated in Mohamed H. Zaki (2021).

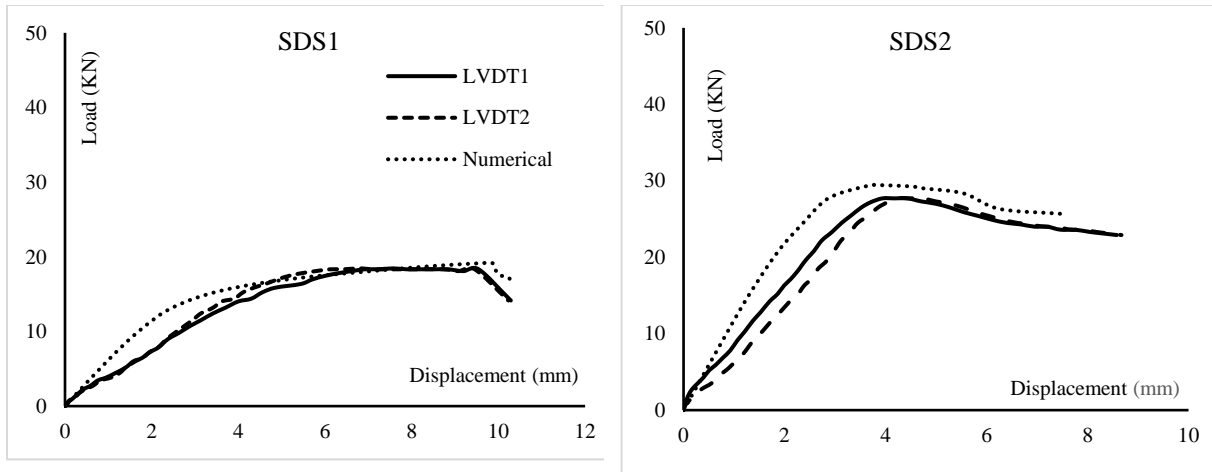


Figure 5: Load-displacement comparison, experimental versus numerical, specimens SDS1, SDS2.

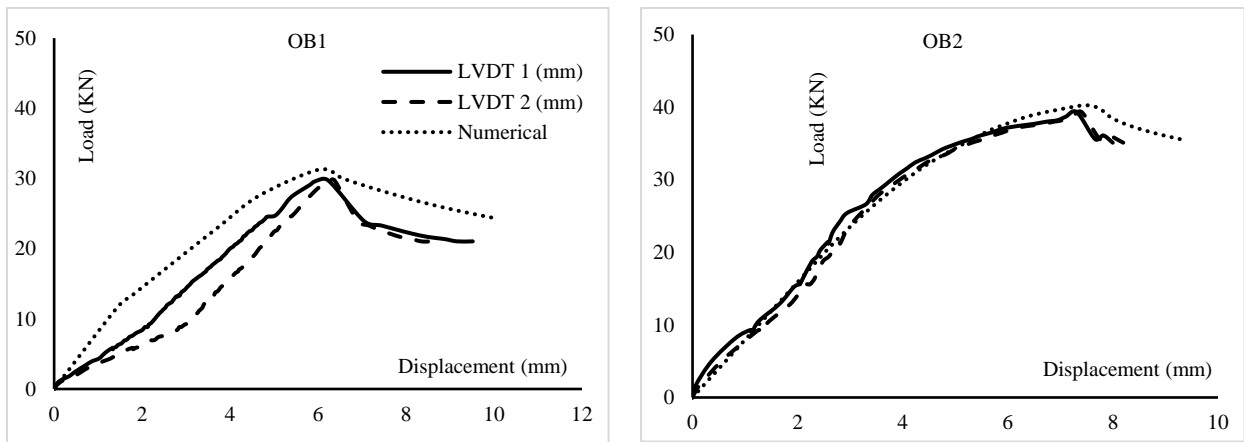


Figure 6: Load-displacement comparison, experimental versus numerical, specimens OB1, OB2.

In this section, the outcomes of the finite element analysis are compared with the experimental test measurements and observations. Fig. 5 and Fig.6 provide comparisons between the experimental and numerical force-displacement pattern of the four specimens. However, Figs. 7 and 8 show the experimental and numerical failure modes. The charts reflect that the ultimate loads obtained from the experimental tests and numerical models are correlated for the four specimens with maximum difference percentage of 6%. Moreover the numerical finite element model deformed shapes at the ultimate loads are similar to the experimental failure modes. The investigation of charts and table explains the close agreement between the two approaches and the ability of numerical model to simulate the behavior of CFS apex connection.

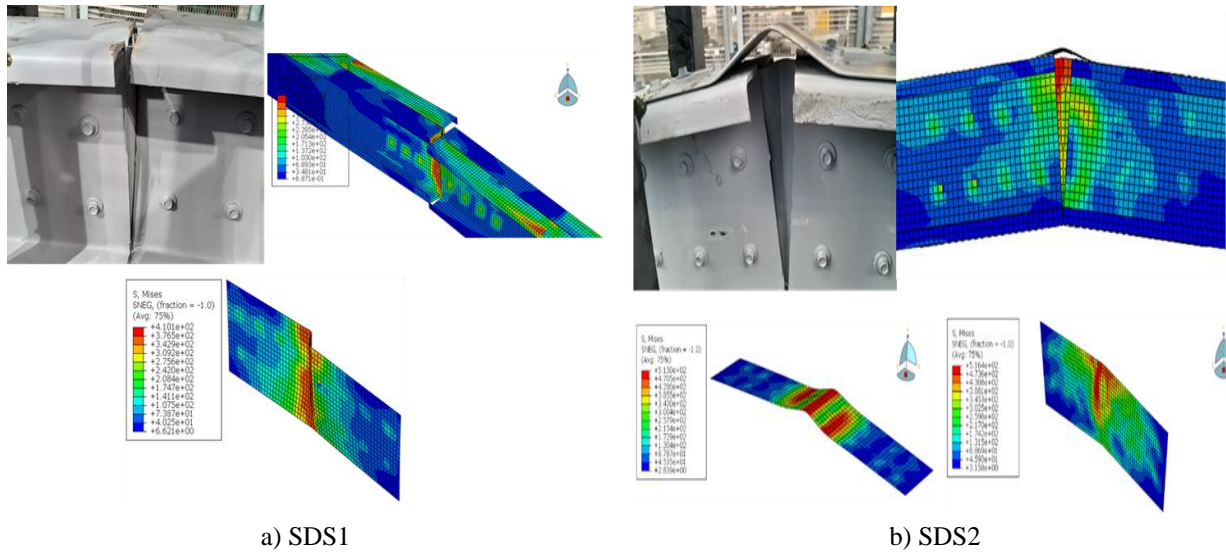


Figure 7: Modes of failure, experimental versus numerical, specimens SDS1, SDS2.

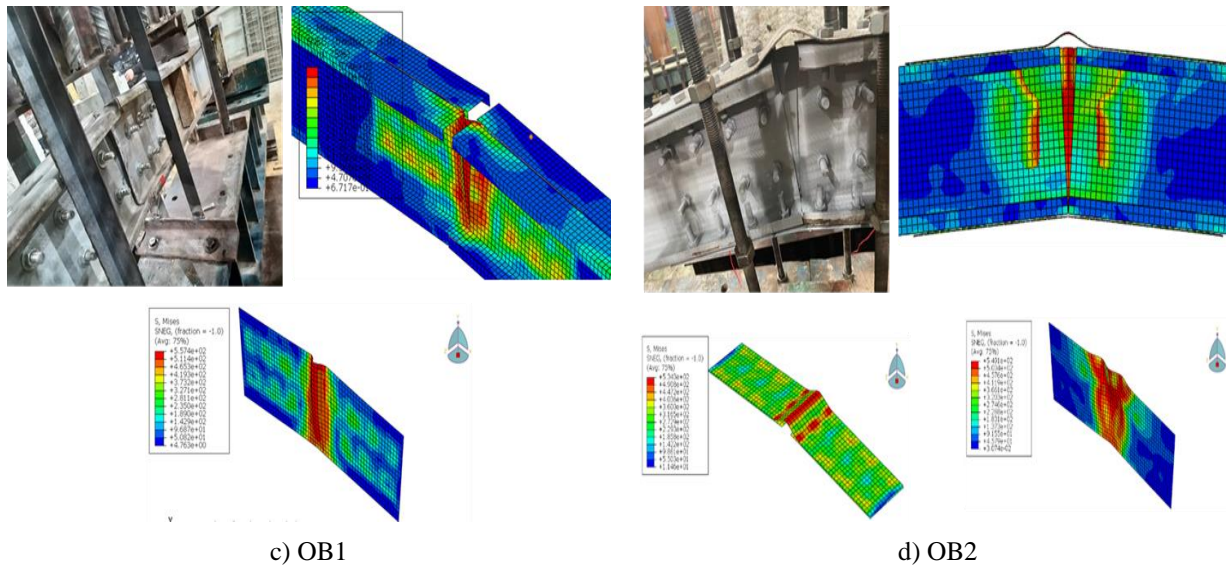


Figure 8: Modes of failure, experimental versus numerical, specimens OB1, OB2.

4. Parametric Study

In this section, a comprehensive parametric study was conducted to investigate the ability to enhance the connection capacity relative to the member's capacity through changing its configuration and dimensions. The effect of each parameter has been studied independently by changing it and keeping all the other parameters unchanged. The parameters included in this study are thickness of gusset plate, number and spacing between self drilling screws, thickness of the cross sections. Table 2 summarizes the specimens that are used to carry out the parametric study with the parameter considered for each specimen.

Table 2. Parametric study variables.

Parameter	Pilot Specimen		Parametric Study	
	ID	Properties	ID	Properties
01- Gusset plate Thickness	SDS1	$t_{gp} = 2 \text{ mm}$	SDS1-1a	$t_{gp} = 1.5 \text{ mm}$
			SDS1-1b	$t_{gp} = 2.5 \text{ mm}$
			SDS1-1c	$t_{gp} = 3 \text{ mm}$
02- Number and Spacing of Screws	SDS1	N=16, S=70 mm	SDS1-2a	N=8, S=150 mm
			SDS1-2b	N=12, S=100 mm
03 – Cold formed section thickness	SDS1	$t_{gp} = 2 \text{ mm}$	SDS1-3	$t_{gp} = 1.5 \text{ mm}$

4.1 Effect of gusset plate thickness

Three different thicknesses of apex gusset plate were used to investigate the effect of changing thickness of gusset plate on the behavior and capacity of CFS apex connections using self-drilling screws. For this purpose, three numerical models were created with specimen ID's SDS1-1a, SDS1-1 b, and SDS1-1 c and gusset plate thicknesses of 1.5, 2.5, and 3 millimeters; respectively and compared to the results obtained for specimen SDS1 with gusset plate thickness equal to 2 mm. Fig. 9 illustrates load-displacement relationship of the cases of study. It is evident that, for specimen SDS1-1a, reducing thickness of gusset plate to 1.5 mm resulted in a significant decrease in the ultimate load by 60% compared to specimen SDS1. However, for specimen SDS1-1b, the ultimate load remained almost the same compared to the original specimen SDS1, while, for specimen SDS1-1c, the ultimate load increased by 16%. It can be concluded that changing the gusset plate thickness has a significant effect on the behavior of the apex connection since the dominant failure mode in SDS1 occurs as local buckling in the gusset plate. Increasing thickness of gusset plate results in increase in the load carrying capacity of the connection as well as the ductility (energy dissipation) of the apex connection.

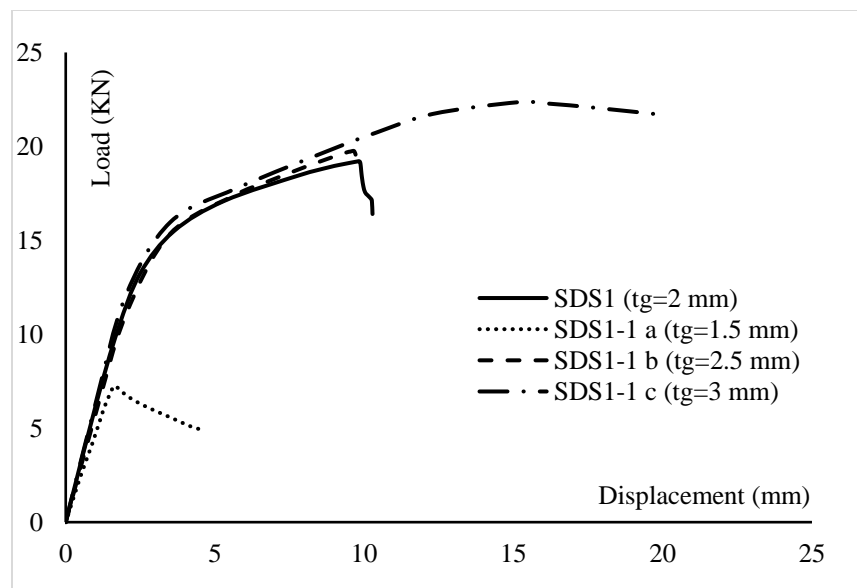


Figure 9: Load-displacement comparison for gusset plate thickness.

4.2 Effect of the number and spacing of fasteners (screws)

In order to investigate the effect of changing number and spacing of self-drilling screws on the behavior of apex connection, two models were created with specimen ID's SDS1-2a (8 screws, 150 mm spacing), and SDS1-2b (12 screws, 100 mm spacing). Then, the results obtained from each model are compared to the results of original specimen SDS1 (16 screws, 70 mm spacing). Connection configuration for each specimen is illustrated in Fig. 10.

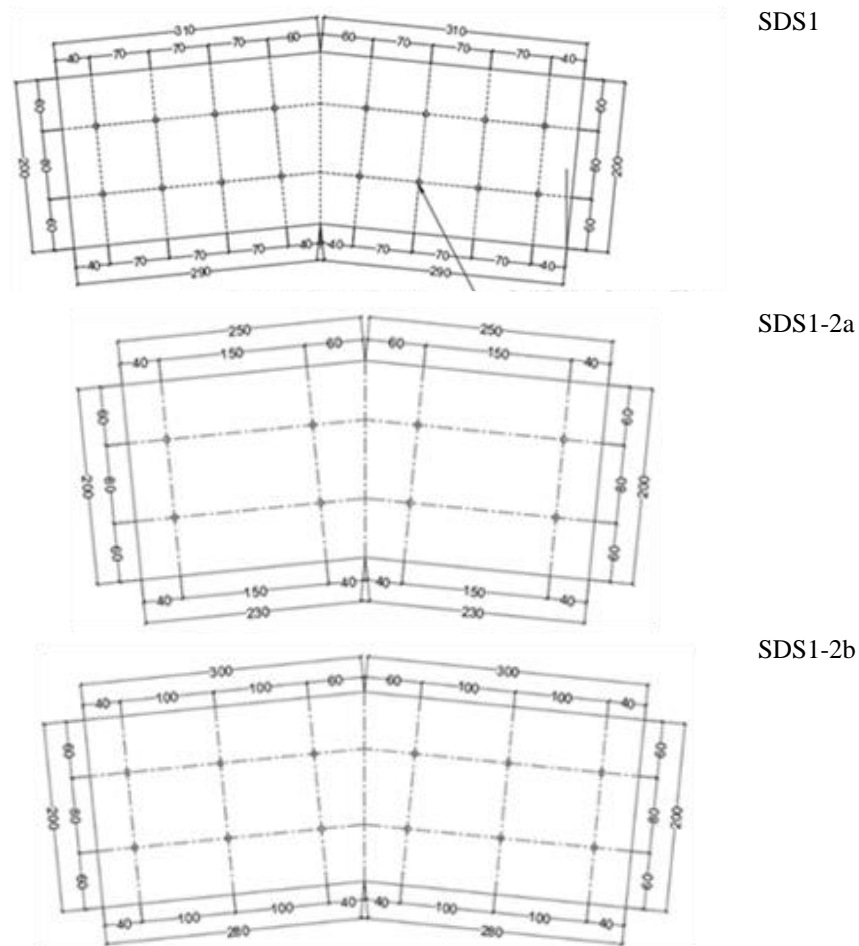


Figure 10: Connection configuration SDS1, SDS1-2a, SDS1-2b.

Load-displacement relations for this study are presented in Fig. 11. It can be noticed that reducing the number of screws and increasing spacing between them results in remarkable decrease in the load carrying capacity of the apex connection. Comparing specimen SDS1-2a (N=8, S=150 mm) to the original specimen SDS1 (N=16, S=70 mm), it is noticed that the ultimate load decreased by 35%. However, for specimen SDS1-2b (N=12, S=100 mm), the ultimate load decreased by 16% compared to SDS1. Thus, increasing number of screws and reducing spacing between them results in increase in the load carrying capacity and decrease in the connection ductility.

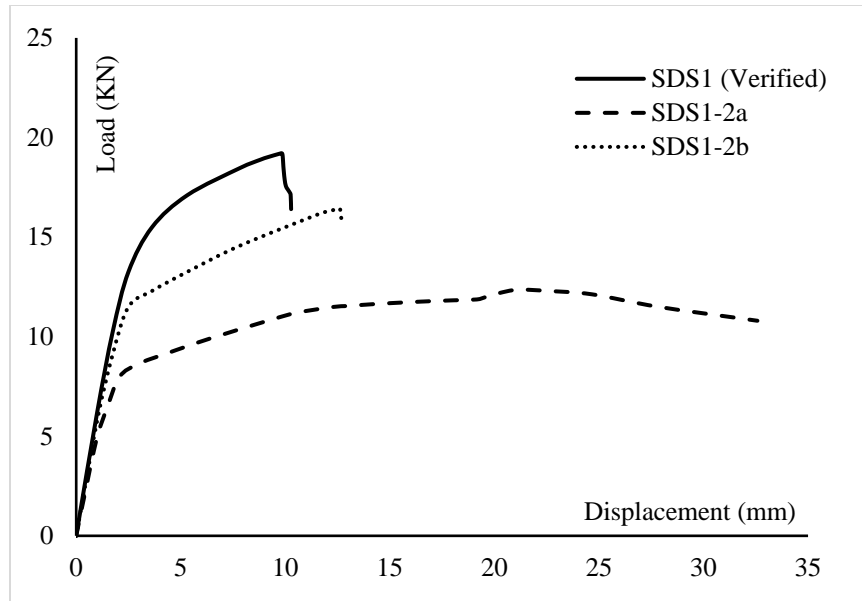


Figure 11: Load-displacement comparison for screw number and spacing.

4.2 Effect of cold formed section thickness

In order to investigate the effect of cross-section thickness on the behavior of apex connection, one model is created with thickness, $t_s = 1.5\text{mm}$ (SDS1-3). Then, the results obtained from this model are compared to the results of original specimen SDS1 ($t_s = 2\text{ mm}$). The load-displacement relations for specimen SDS1-3 compared to the original specimen SDS1, and stress distribution as well as deformed shape on each specimen are depicted in Figs.12, 13, 14; respectively. is illustrated in Fig.14.

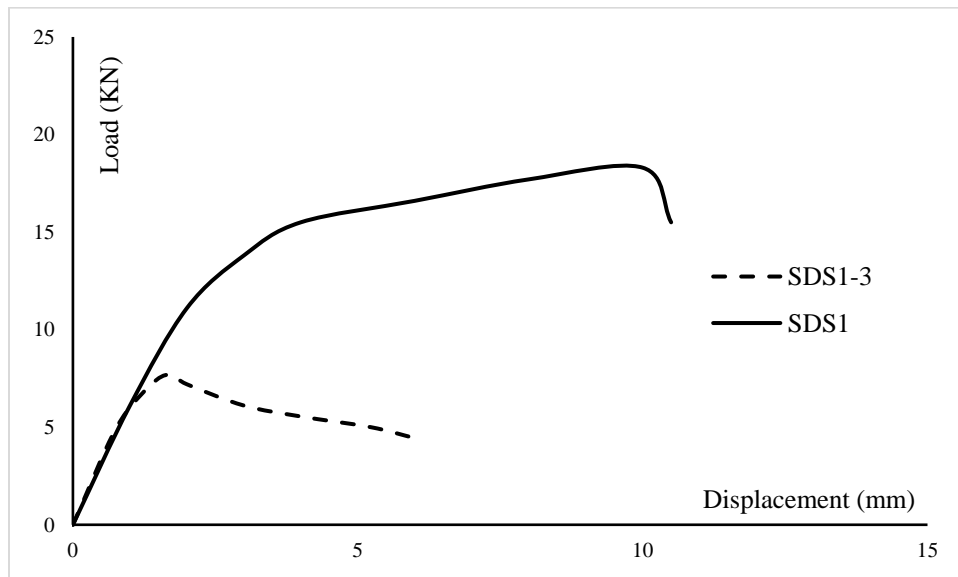


Figure 12: Load-displacement comparison of SDS1 versus SDS1-3.

It can be noticed that the structural behavior of the specimens remained the same, where failure occurred as local buckling in the gusset plates of the specimens. Moreover, reducing thickness of cross-section hugely reduced the load carrying capacity of the apex connection, by 60%.

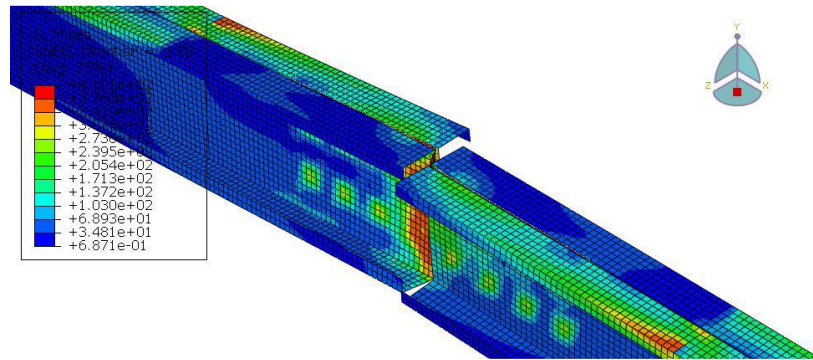


Figure 13: Stress distribution and deformed shape of specimen SDS1, $t=2\text{mm}$.

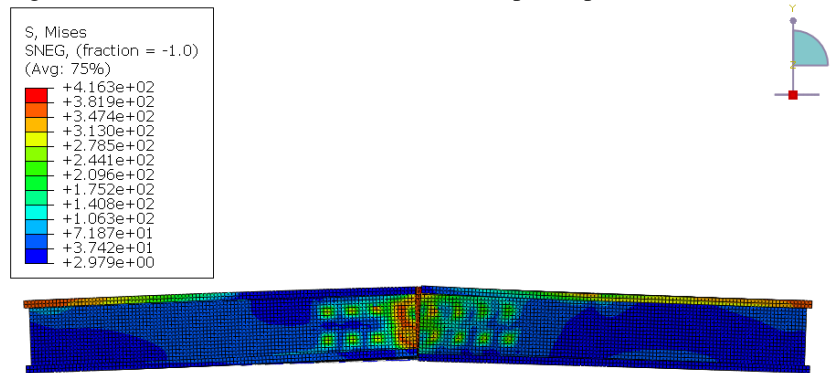


Figure 14: Stress distribution and deformed shape of specimen SDS3, $t=1.5\text{mm}$.

5. Conclusions

In this study, the behavior of cold formed steel portal frame apex connection subjected to major axis bending moments is investigated. For this purpose, experimental and numerical models were developed. Based on the experimental work, numerical models and the parametric study, the following conclusions may be drawn:

- The dominant failure mode was local buckling of the connection plate elements that are subjected to compression. The failure of cross-section was rarely noticed outside the gusset plate zone.
- The use of upper and lower plates to connect the CFS flanges in addition to the gusset plate that connecting the web increased the flexural capacity of the apex connection by about 33%.

- In terms of the connection moment capacity compared to the moment capacity of the cross-section, bolted specimens achieved high ratios compared with the self-drilling screws.
- Increasing thickness of gusset plate resulted in a considerable increase in the ultimate load carrying capacity of apex connection as well as the connection ductility and energy dissipation. The main reason was that the dominant failure mode of apex connection was the buckling of gusset plate.
- The number and spacing of screws had a remarkable influence on the structural behavior of apex connections. Increasing the number of screws while reducing spacing between them resulted in a significant increase in the ultimate load carrying capacity of the connection. However, the connection ductility decreased. This may be attributed to the increase in connection rigidity with increasing number of screws.
- Thickness of cross-section had a significant effect on the ultimate load carrying capacity as well as the ductility of the apex connection.

References

- AISI S100-12. North American specifications for the design of cold-formed steel structural members. North American cold-formed steel specification. Washington, DC: American Iron and Steel Institute; 2012.
- Abaqus, G. (2011). Abaqus 6.11. Dassault Systemes Simulia Corporation, Providence, RI, USA.
- ASTM A370, A370-06 (2006), Standard Test Methods and Definitions for Mechanical Testing of Steel Products, American Society for Testing and Materials.
- Blum, H. B., & Rasmussen, K. J. R. (2019). "Experimental and numerical study of connection effects in long-span cold-formed steel double channel portal frames". *Journal of Constructional Steel Research*, 155, 480-491.
- Blum, H. B., & Li, Z. (2019). "Stability of apex connections in cold-formed steel portal frames. *Proceeding of the Annual Structural Stability Research Council Conference, SSRC 2019* (pp. 548-560).
- Badr, A. R., Elanwar, H. H., & Mourad, S. A. (2019). "Numerical and experimental investigation on cold-formed walls sheathed by fiber cement board". *Journal of Constructional Steel Research*, 158, 366-380.
- Chen, X., Blum, H. B., Roy, K., Pouladi, P., Uzzaman, A., & Lim, J. B. (2021). "Cold-formed steel portal frame moment-resisting joints: Behaviour, capacity, and design". *Journal of Constructional Steel Research*, 183, 106718.
- Calderoni, B., De Martino, A., Formisano, A., & Fiorino, L. (2009). "Cold formed steel beams under monotonic and cyclic loading: Experimental investigation". *Journal of Constructional Steel Research*, 65(1), 219-227.
- European Standard EN 1993-1-3, Eurocode 3. Design of steel structures – Part 1–3: general rules-supplementary rules for cold-formed thin gauge members and sheeting. Brussels: European Committee for Standardization (CEN); 2001.
- El-Hadary, M. R., El-Aghoury, I. M., & Ibrahim, S. A. B. (2021). "Behavior of different bolted connection configurations in frames composed of cold-formed sections". *Ain Shams Engineering Journal*.
- Elkersh, I. (2010). "Experimental investigation of bolted cold formed steel frame apex connections under pure moment". *Ain Shams Engineering Journal*, 1(1), 11-20.
- Egyptian Code of Practice for Steel Construction and Bridges (Allowable Stress Design), Code no. ECP 205, 2016 Edition.
- Hanna, M. T., El-Saadawy, M. M., M El-Mahdy, G., & Aly, E. H. (2018). "Behavior of Beam to Column Cold-Formed Section Connections Subjected to Bending Moments". *International Specialty Conference on Cold-Formed Steel Structures*, St. Louis; United States.
- Huynh, M. T., Pham, C. H., & Hancock, G. J. (2020). "Design of screwed connections in cold-formed steels in shear". *Thin-Walled Structures*, 154, 106817.
- Lim, J. B., & Nethercot, D. A. (2004). "Stiffness prediction for bolted moment-connections between cold-formed steel members". *Journal of constructional steel research*, 60(1), 85-107.

- Meza, F. J., Becque, J., & Hajirasouliha, I. (2020). "Experimental study of the cross-sectional capacity of cold-formed steel built-up columns". *Thin-walled Structures*, 155, 106958.
- Mohamed H. Zaki (2021). "Laboratory Testing and numerical Modelling of Frame apex connections fabricated from steel cold-formed sections", *A Thesis Submitted to the Faculty of Engineering at Cairo University in Partial Fulfillment of the Requirements for the Degree of master of science in Structural Engineering*, Cairo
- Öztürk, F., & Pul, S. (2015). "Experimental and numerical study on a full-scale apex connection of cold-formed steel portal frames". *Thin-Walled Structures*, 94, 79-88.
- Rasmussen, K. J. (2019). "Behaviour and modelling of connections in cold-formed steel single C-section portal frames". *Thin-Walled Structures*, 143, 106233.
- Roy, K., Lau, H. H., Ting, T. C. H., Masood, R., Kumar, A., & Lim, J. B. (2019). "Experiments and finite element modelling of screw pattern of self-drilling screw connections for high strength cold-formed steel". *Thin-Walled Structures*, 145, 106393.
- Tshuma, B., & Dundu, M. (2017). "Internal eaves connections of double-bay cold-formed steel portal frames". *Thin-Walled Structures*, 119, 760-769.
- Ye, J., Mojtabaei, S. M., Hajirasouliha, I., Shepherd, P., & Pilakoutas, K. (2018). "Strength and deflection behaviour of cold-formed steel back-to-back channels". *Engineering Structures*, 177, 641-654.